Partial Safety Factors in Pile Bearing Capacity

Portance des Pieux: Facteurs Partiels de Sécurité

E. De BEER Professor, State University Ghent, Belgium
E. LOUSBERG Professor, Université de Louvain, Louvain-la-Neuve, Belgium
A. de JONGHE Inspector General, Ministry of Public Works, St.-Niklaas, Belgium
M. WALLAYS Head R-D Department, Franki International, Liège, Belgium
R. CARPENTIER Chief Engineer, Geotechnical Institute, Ghent, Belgium

SYNOPSIS From an extensive study of loading tests on piles with different base diameter in a stiff fissured clay and at a shallow depth in a dense sand it is deduced that the allowable bearing capacity can be obtained from the ultimate bearing capacity, forecast from the results of CPT tests, by applying partial safety factors, one F_1 covering the problem of large deformations and the others η_1 and η_2 covering the dispersion, resp. for base and lateral bearing capacities.

INTRODUCTION

For determining the allowable load on displacement piles from the ultimate base and lateral bearing capacities, deduced from CPT tests, a safety margin has to be taken into account. This safety margin must guarantee that the allowable load is located outside the zone of large deformations, and must cover the dispersion of the mechanical properties of the soil from one vertical to another.

Instead of characterizing this safety margin by the introduction of a unique factor, it is proposed to apply partial factors, one F_1 covering the problem of the large deformations, the others η_1 and η_2 covering the dispersion respectively for base and lateral bearing capacities.

In Belgium, for an oligocene clay formation and for a pliocene sand formation, starting from extended pile testing programs and from a systematic analysis of all available data, the values of the above mentioned safety factors have been deduced.

PRINCIPLES OF THE METHOD

The ultimate bearing capacity Q_r of a displacement pile can be written as

$$Q_r = Q_{b,r} + Q_{s,r} \tag{1}$$

with

$Q_{b,r}$ = the ultimate bearing capacity at the base

$Q_{s,r}$ = the ultimate bearing capacity by skin friction.

Methods exist to predict the values of $Q_{b,r}$ and $Q_{s,r}$ for displacement piles from the results of CPT tests (De Beer, 1971/72 ; De Beer et al., 1977).

For the determination of the allowable bearing capacity two cases have to be considered :

a) the pile is driven at the vertical of a previously performed CPT test
b) the pile is driven outside the verticals of performed CPT tests.

a) In the rather exceptional case that at the vertical of each pile to be driven, previously a CPT test should have been performed, a safety factor F_1 is to be applied with the only aim to locate the allowable load outside the zone of the load-settlement diagram where the settlements increase rapidly with the imposed loads

$$Q_a = \frac{Q_r}{F_1} \tag{2}$$

b) In the more general case, for the whole of the piles of a foundation, only a limited number of CPT tests are at disposal. If now the allowable bearing capacity is to be defined not from a CPT test performed at the vertical of the pile itself, but from a certain number of tests performed over the area of the construction, care must be taken of the influence of the scatter of the soil properties from one vertical to another.

If over a sufficiently large testing area (for instance 10.000 m^2) of a given geological formation, a sufficiently large number of CPT tests have been performed, from these tests maximum, respectively minimum values of $Q_{b,r}$ and $Q_{s,r}$ can be determined. From these values the following ratios can be calculated

$$\eta_1 = \left(\frac{Q_{b,r,max}}{Q_{b,r,min}}\right)_{\text{test site}} \tag{3}$$

$$\eta_2 = \left(\frac{Q_{s,r,max}}{Q_{s,r,min}}\right)_{\text{test site}} \tag{4}$$

If now a problem has to be solved in anoter area of the same formation, on the basis of a limited number of CPT tests, one can determine from these tests the values $Q_{b,r,max}$, $Q_{s,r,max}$, $Q_{b,r,min}$ and $Q_{s,r,min}$.

The allowable bearing capacity Q_a is then given by

$$Q_a = Q_{a,1} = \frac{1}{F_1}\left(\frac{Q_{b,r,max}}{\eta_1} + \frac{Q_{s,r,max}}{\eta_2}\right) \tag{5}$$

with η_1 and η_2 the values defined from the test site.

A condition however is that $Q_{a,1}$ is not larger than

$$Q_{a,1} \leq Q_{a,2} = \frac{1}{F_1} (Q_{b,r,min} + Q_{s,r,min}) \qquad (6)$$

If this condition is not satisfied it shows that the dispersion of the soil properties at the building site is larger than on the test site, and therefore that supplementary CPT tests have to be performed in order to better define the variance of the soil properties, with the aim to divide the building site in more homogeneous partial areas.

The outlined general principles will be applied to two Belgian geological formations.

OLIGOCENE STIFF FISSURED CLAY FORMATION (RUPELIAN - BOOM CLAY)

Test site

At Kontich an extended pile testing program has been performed in the Boom clay which is a stiff fissured clay of oligocene age (Rupelian). The results of the test program have been fully described by De Beer et al. (1977).

The characteristics of the test piles are given in fig. 1.

At the vertical of each pile a CPT test M4 was previously performed.

An important observation with stiff fissured clays is the dispersion of the test results as well as for the cone resistance as for the total side friction from one vertical to anoter.

This is illustrated by fig. 2 giving the dispersion for 2 nearby CPT tests M4 performed in the Boom clay at Kontich.

For the London clay, Marsland (1974) found similarly that the regression lines of cone resistances versus depth are different from one vertical to another and that most do not intersect, showing that along some verticals systematically lower resistances are found than along others.

The cause of such an important dispersion has not yet been clarified. However one must conclude that the observed dispersion should be in essence related to the variability of the mechanical properties of the clay from one vertical to another.

The ultimate bearing capacities Q_r^{calc} of the test piles, calculated with the method described by De Beer et al. (1977) starting from the results of the CPT tests previously performed at the vertical of each pile, are given in fig. 1.

The allowable loads, obtained by applying a safety factor F_1 = 1,4, and the corresponding settlements are also given in fig. 1. It appears that by applying a safety factor F_1 = 1,4 on Q_r^{calc}, the allowable load is located outside the zone of the load-settlement diagram where the settlements increase rapidly with the imposed loads. As an example this is illustrated for the piles II, VII and IX in fig. 3.

At Kontich for piles with a shaft length of 10 m, but with different bases (fig. 1) the value of η_1 varies with the type of pile between 1,44 and 1,54.

When considering piles with the same diameter D_b = 406 mm but with lengths of 7 m and 13 m, the value of η_1 varies between 1,57 and 1,50.

Thus for the clay at Kontich a value 1,5 for η_1 can be adopted.

For the 16 CPT tests at Kontich, considering a shaft Ø 406 mm with a length of 10 m, a value η_2 = 1,27 is found. Therefore a value η_2 = 1,30 can be adopted.

Thus the statistical scatter of the Boom clay at Kontich is characterized by η_1 = 1,5 for the resistance at the base, and η_2 = 1,3 for the total side friction.

Application outside the test site

It is of course of primary importance to know beforehand if the degree of scatter found at Kontich is characteristic for most of the Boom clay formation, or if at the contrary it must be expected that in several places of this formation the scatter can be larger.

In order to check if the scatter factors η_1 and η_2 have a general meaning for the whole Boom clay formation, a systematic review has been made of all the CPT tests performed in the Boom clay, especially in the region of Antwerp, where this clay is found at relatively small depths. For 22 different construction sites the approximate values of η_1 and η_2 have been deduced.

For the sake of simplicity the value of η_1 has not been calculated as the ratio $Q_{b,r,max} : Q_{b,r,min}$ for a given pile, but as the ratio $q_{c,max} : q_{c,min}$ and that for every depth. Because of the much more important fluctuations of $q_{c,max} : q_{c,min}$, this ratio constitutes an upper limit of the ratio $Q_{b,r,max} : Q_{b,r,min}$.

For η_2, because of the variable thickness of the superficial layers covering the Boom clay, not the absolute values of the total side friction Q_{st}, but the increases of Q_{st} starting from the depths where the total side friction diagram becomes nearly linear, have been considered.

In table I for each of the considered sites, and eventually for zones of the sites, after analyzing the graphs at disposal, the mean values obtained for η_1 and η_2, the number of tests at disposal, the radius of the concerned zone, and eventual comments are given.

For the 22 examined sites η_1 resp. η_2 are smaller than or practically of the order of magnitude of 1,5 resp. 1,3 except for two special cases.

On the site N° 19, two cone penetration tests distant of 12 m, show increases of the total side friction which differ by a factor of 2. On the other hand, these tests show that over a relatively small distance, the upper face of the Boom clay shows a level difference of 1,80 m. Such a large level difference can only be explained by a special geological feature (diapir), which has caused an important local variation of the properties of the clay.

At the site N° 22, located along the right bank of the Scheldt river, 55 CPT tests over an area of several hectares are available. These tests have been grouped according to the location of the different constructions. For the zones located sufficiently far away from the riverbank the values of the ratios η_1 and η_2 correspond practically with the values at Kontich. At the contrary, for the test sites located immediately along the bank of the Scheldt

TABLE I

Site N°	Construction site	Number of C.P.T. tests	Radius of zone m	n_1	n_2	Comments
1	Putte	4	50	1,44	1,21	-
2	Hoboken	4	40	1,49	1,37	-
3	Duffel	2	20	1,12	1,10	-
	St.Kat.Waver					
4	RM.10	4	30	1,24	1,08	-
5	RM.11	4	30	1,26	1,34	-
6	RM.12	6	30	1,37	1,11	(1)
7	RM.14	4	30	1,47	1,26	-
	Antwerpen					
8	Blancefloer-laan	6	50	1,31	1,17	-
9	E3 4826	12	100	1,29	(1,63)	(2)
10	E3 2448	7	30	1,21	1,25	-
11	E3 KM48	9	30	1,38	1,21	-
12	E3 KM26	5	50	1,24	(1,52)	(3)
13	E3 8446 N	4	10	1,2 } 1,62	1,24	(4)
	S	3	10	1,42		
14	E3 2682	2	20	1,15	1,09	-
15	E3 2426 N	3	10	1,43	1,10 } 1,54	(4)
	S	6	10		1,33	
16	E3 8426 N	3	10	1,20 } 1,59	1,21	(4)
	S	3	10	1,25		
17	E3 8482	3	30	1,22	1,44	-
18	E3 64SR N	3	10	1,26	1,05 } 1,50	(4)
	S	4	10		1,05	
19	E3 42SR + 48SR	11	50	1,47	(2,26)	(5)
20	Boom	20	900	1,5 (z<9,00m) 1,7 (z>9,00m)	1,25	-
21	Hoboken I'-V'	5	75	1,49	1,34	(1)
22	Cockerill					
	I - VI	6	20	1,45	1,37	(1)
	VII - XXVIII	21	75	(3,1)	(1,62)	(6)
	XXVIII - XXI	11	80	1,41	1,29	(1)

Comments

(1) two layers in the clay, the upper layer seems altered; the given values correspond to the lower layer ;

(2) marked difference of the values of Q_{st} when just entering the clay ;

(3) level uncertain, probably diapir ;

(4) because of systematic differences, several zones have been considered ;

(5) probable occurrence of a diapir ;

(6) alteration due to the proximity of the Scheldt river.

river, the dispersion of these ratios is much larger. This dispersion is to be linked to the proximity of the Scheldt river.

The systematic exploitation of the data at disposal shows that, when excepting local accidents due to the geology or/and the morphology of the soil, factors n_1 = 1,5 and n_2 = 1,3 defining the heterogeneity of the soil for the base resistance and the total side friction, have a general meaning for the Rupelian clay, in as far as zones are considered whose extension is limited to about 100 m.

DENSE PLIOCENE SAND FORMATION (SCALDISIAN-SAND OF KALLO)

Test site

At Kallo a series of test piles were driven through soft upper layers into a very dense sand layer of pliocene age (Scaldisian-Sand of Kallo). The results of the test program have been described by De Beer et al. (1979a ; 1979b).

The characteristics of the test piles are given in fig. 4.

At the vertical of each pile a CPT test M4 was previously performed, showing similar results as well for the cone resistance as for the total side friction from one vertical to another. The results of CPT test III are given in fig. 5 as an example.

The ultimate bearing capacities Q_r^{calc} of the test piles, calculated with the method described by De Beer (1971/72) starting from the results of the CPT tests previously performed at the vertical of each pile, are given in fig. 4.

The allowable loads Q_a, obtained by applying a safety factor F_1 = 1,4, and the corresponding settlements are also given in fig. 4. Also for the pliocene sand formation it appears that by applying a safety factor F_1 = 1,4 on the calculated ultimate bearing capacity Q_r^{calc}, the allowable load is located outside the zone of the load-settlement diagram where the settlements increase rapidly with the imposed loads. This is illustrated for the seven test piles in fig. 6.

Considering a pile with a given base diameter and a given depth successively at the location of the different CPT tests, the dispersion factor n_1 varies in function of the considered diameter and the considered depth between 1,24 and 1,34.

At the test site the soft upper layers have practically in each vertical the same thickness and the same composition. For that reason, at the test site it is possible to consider and to compare the total side friction. For this total side friction a maximum scatter n_2 = 1,3 was found.

Thus for the tested piles the statistical scatter of the Sand of Kallo at the test site is characterized by n_1 = 1,3 for the unit base resistance and by n_2 = 1,3 for the total side friction.

Determination of the dispersion factors n_1 and n_2 outside the test site

For the Western extension of the Antwerp Harbour, over an area of some 35 km², in the zone of existence of the sand of Kallo, about 250 CPT tests have been performed, however mostly at mutual distances larger than 200 m. Over this area from one place to another the thickness of the upper layers above the sand of Kallo, can be very different and also their composition. As the aim is to determine the dispersion factors on unit base bearing capacity and side friction for piles in groups with an area not larger than about 100 m x 100 m, of course characterized by about the same thickness and composition of the upper layers, it is necessary to classify the tests according to those criteria.

Dispersion factor n_1 for unit base bearing capacity

To determine the dispersion factor n_1, a reference pile with D_b = 600 mm, ended at relative depths of 2 D_b to 3 D_b in the dense sand has been considered.

As the difference in thickness and in composition of the upper layers influences the base bearing capacity of a pile penetrating at a relatively small depth into the very dense sand, a subdivision of the considered CPT tests was made into 6 groups characterized by the limits of the unit base bearing capacity $q_{b,r,o}$ just above the very dense sand layer, given in table II.

TABLE II

Dispersions e_1 for the different groups

Group	Depth 2 D_b		Depth 3 D_b	
$q_{b,r,o}$ MN/m^2	e_1	L_{Mm} in km	e_1	L_{Mm} in km
0-1,5	1,737	2,67	1,673	3,56
1,5-2,5	1,602	3,45	1,505	3,53
2,5-3,5	1,525	3,13	1,646	3,47
3,5-5,5	1,570	3,16	1,842	3,02
5,5-8,0	1,550	4,67	1,566	4,67
> 8,0	1,354	0,91	1,313	0,91

central value : 1,57

The dispersions e_1 for the considered groups are given in table II ; they vary between 1,313 and 1,842, with a central value of 1,57.

In the same table, for each group are given the distances L_{Mm} between the tests giving the maximum and minimum values.

All these characteristic distances are much larger than 100 m. In fact most of the groups cover the total tested area. If now only an area of 100 m x 100 m has to be considered, doubtless the dispersions will be much lower, and therefore considering the values found for e_1 for such a limited area a value of $\eta_1 \leqslant 1,50$ can be expected.

Dispersion factor η_2 for the unit side friction in the dense sand

As can be seen from fig. 5, because of the high resistances encountered in the dense sand layer, in order to be able to enter sufficiently deep in that layer, it becomes rapidly necessary to reduce artificially the side friction, with the consequence that in several tests, from a rather small depth on in the sand layer, the exact value of the side friction is unknown. Furthermore in several other tests the total side friction diagram has a very irregular shape, in which locally there is practically no increase of the side resistance, at depths with large cone resistances. For both reasons, in the dense sand layer, the use of the total side friction diagram is impossible or questionnable.

Therefore, for determining the value of the unit side friction, use was made of data relating this unit side friction to the cone resistance (Te Kamp, 1977 ; Van den Elzen, 1979). In the present case, for a steel tube the value $\tau_s = q_c : 200$ was used.

Considering a penetration depth of 3 m, a mean value f of the τ_s values over this depth can be obtained.

The distribution curve of f for the N = 251 tests is given on fig. 7, and the cumulative curves $\eta = \frac{n}{N}$ and $y = \Sigma n \, \Delta f$ versus f are given on fig. 8 and 9.

From a probabilistic analysis it appears that the deviation z over the total area A = 35 km², can be expressed by a log normal function

$$z = a \log \frac{f}{f_r} \qquad (7)$$

With a = 25,41
f_r = central value = 129 kN/m²
h = concentration factor = 0,443
E_q = mean quadratic deviation = 1,596.

The probability that the dispersion $m = f_{max} : f_{min}$ should be less than 1,3 is 65 %. For a dispersion $m = f_{max} : f_{min} =$ 1,5 the probability increases to 82,5 %. Therefore over an area of 35 km², the probability that the unit friction resistance f should be located between $0{,}87 . f_r$ = 0,87 x 129 = 112 kN/m² and 1,13 x 129 = 146 kN/m² is 65 % and that it should be located between 0,8 x 129 = 103 kN/m² and 1,2 x 129 = 155 kN/m² is 83 %.

If now instead of an area of 35 km², much smaller partial areas with an order of magnitude of 10^{-2} km² are considered a much better concentration around the central value can be expected.

For instance for the test site with an area of 5 x 10^{-4} km², a concentration factor h = 1,772 and mean quadratic deviation E_q = 0,333 are obtained, with the consequence that the probability of a dispersion $m = f_{max} : f_{min} = 1{,}3$ is practically equal to unity.

From all these results it can be deduced that for an arbitrary surface not larger than 10^{-2} km² there is a fair probability that the ratio of the maximum unit friction resistance in the dense sand, to the minimum unit friction resistance, will be smaller than 1,3, and a very larger probability that it will be smaller than 1,5.

ACKNOWLEDGEMENT

The research was performed by S.A. Pieux Franki and was sponsored by the Belgian Governmental Institute for Scientific Research in Industry and Agriculture.

The test sites were put at the disposal by the Ets. Moorkens and by the Ministry of Public Works.

REFERENCES

De Beer, E.(1971/72). Méthodes de déduction de la capacité portante d'un pieu à partir des résultats des essais de pénétration. Annales des Travaux Publics de Belgique, 4, 5, 6.

De Beer, E., Lousberg, E., Wallays, M., Carpentier, R., De Jaeger, J. and Paquay, J. (1977). Bearing capacity of displacement piles in stiff fissured clays. Comptes Rendus de Recherches, 39, IRSIA-IWONL, Brussels.

De Beer, E., Lousberg, E., De Jonghe, A., Carpentier, R., Wallays, M. (1979a). Analysis of the results of loading tests performed on displacement piles of different types and sizes penetrating at a relatively small depth into a very dense sand layer. Proc. Conf. Recent Developments in the Design and Construction of Piles, 139-151, ICE, London.

De Beer, E., Lousberg, E., De Jonghe, A., Wallays, M., Carpentier, R. (1979b). Prediction of the bearing capacity of displacement piles penetrating into a very dense sand layer, from the results of CPT tests. Proc. 7th E. Conf. Soil Mech. Found. Eng., (3), 51-59, Brighton.

Marsland, A. (1974). Comparisons of the Results from Static Penetration Tests and Large in Situ-Plate Tests in London Clay. Building Research Establishment. Current paper CP 87/74.

Te Kamp, W. (1977). Sonderen en funderingen op palen in zand. Sondeersymposium Fugro, Leidschendam, NL., 121-132.

Van den Elzen, L. (1979). Concrete screw piles, a vibrationless, non displacement piling method. Proc. Conf. Recent Developments in the Design and Construction op Piles, 67-71, ICE, London.

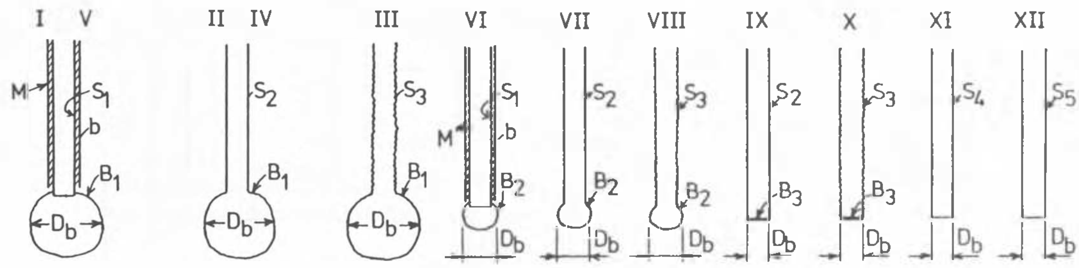

	I V	II IV	III	VI	VII	VIII	IX	X	XI	XII
D_b (m)	I 1,398 V 1,410	II 1,482 IV 1,420	1,446	0,624	0,636	0,632	0,406	0,406	0,406	0,406
$Q_r^{(e)}$ (MN)	I 1,94 V 2,20	II 3,01 IV 3,15	3,33	0,58	1,49	2,12	0,82	1,15	0,96	0,87
Q_r^{calc} (MN)		II 2,67 IV 2,79	3,22		1,33	1,78	0,90	1,25	0,94	0,88
$\frac{Q_r^{calc}}{1,4}$ (MN)		II 1,91 IV 1,99	2,30		0,95	1,27	0,64	0,89	0,67	0,63
s (mm)		II 7,09 IV 7,72	8,99		4,06	4,26	4,47	4,80	3,13	3,33

Length of shaft 10 m ; Diameter of shaft 0,406 m

B_1 : overexpanded Franki base - B_2 : normal enlarged Franki base - B_3 : steel plate

S_1 : prefab shaft - S_2 : vibrated shaft - S_3 : Franki shaft made by hammering - S_4 : prefab concrete pile with smooth shaft, introduced by hammering - S_5 : prefab pile with steel jacket, introduced by hammering

M : floating steel mantle - b : bentonite slurry.

Fig.1 Types of piles tested at Kontich in Boom clay

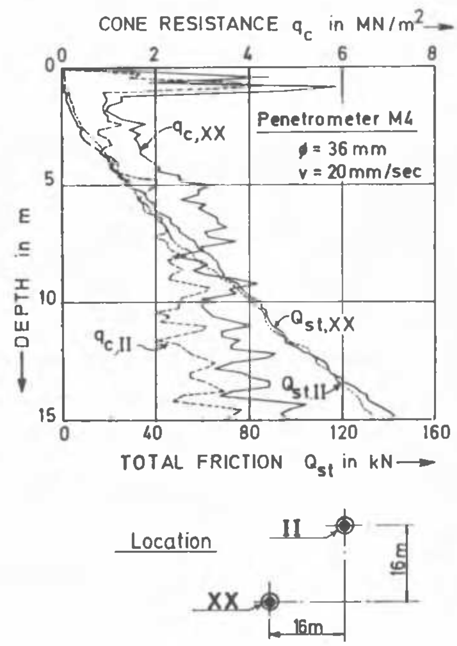

Fig.2 Dispersion of CPT test results at Kontich (distorted scale)

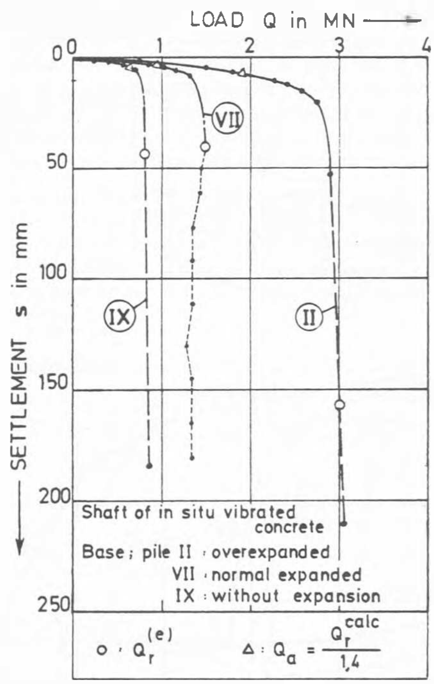

Fig.3 Load settlement diagrams of test piles II, VII and IX at Kontich

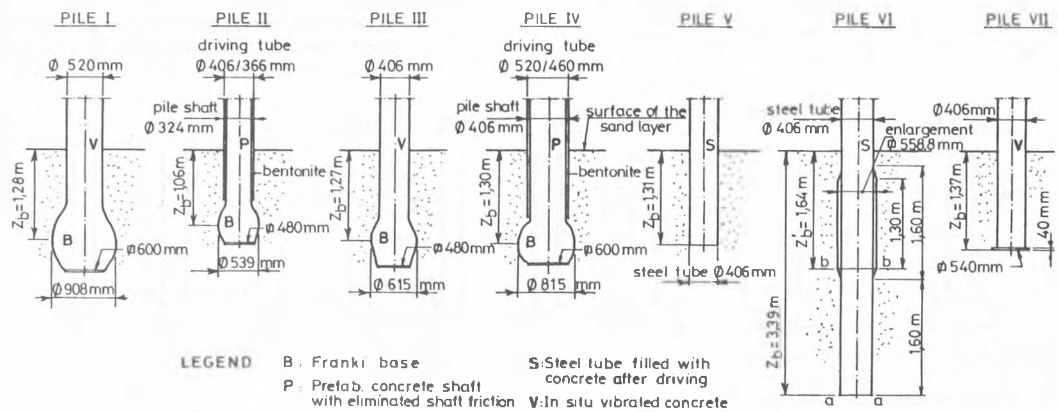

	PILE I	PILE II	PILE III	PILE IV	PILE V	PILE VI	PILE VII
Q_ℓ (MN)	4,76	2,55	2,70	4,41	1,47	3,97	2,40
Q_r^c (MN)	6,08	2,70	3,19	5,20	1,67	4,51	2,80
Q_r^{calc} (MN)	4,54	2,12	2,71	4,06	1,30	4,14	2,49
$\frac{Q_r^{calc}}{1,4}$ (MN)	3,24	1,51	1,94	2,90	0,93	2,96	1,78
s (mm)	11,96	7,57	10,32	9,45	6,70	9,87	19,74

Fig.4 Types of piles tested at Kallo in dense sand

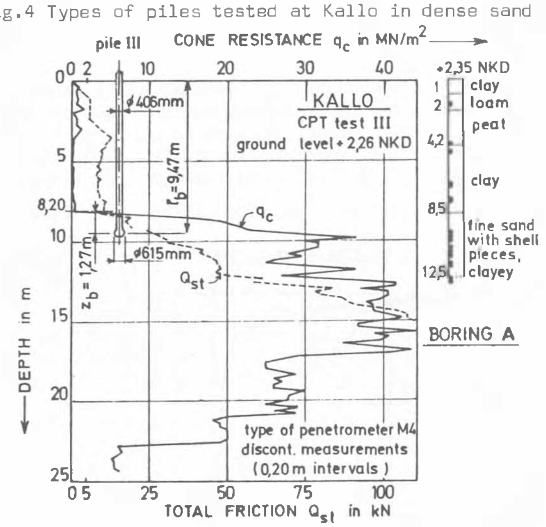

Fig.5 CPT test III at Kallo

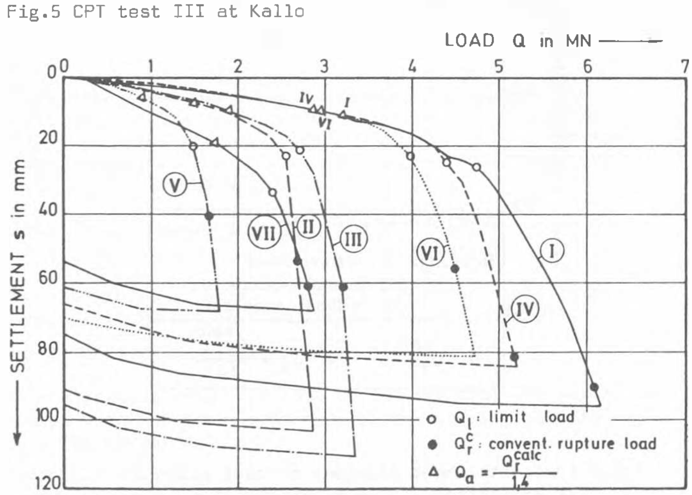

Fig.6 Load settlement diagram of test piles at Kallo

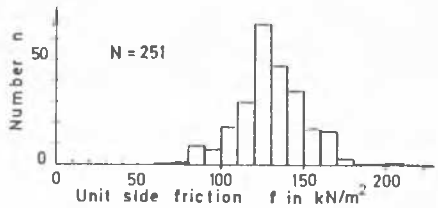

Fig.7 Distribution of f in the sand of Kallo

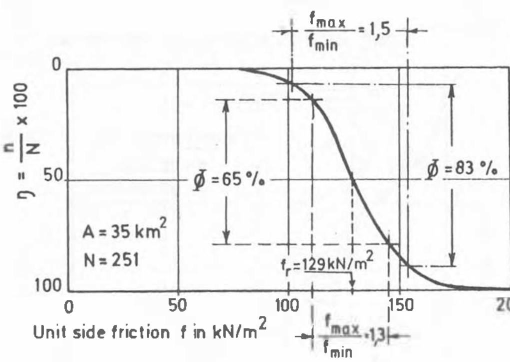

Fig.8 Cumulative curve of f in the sand of Kallo

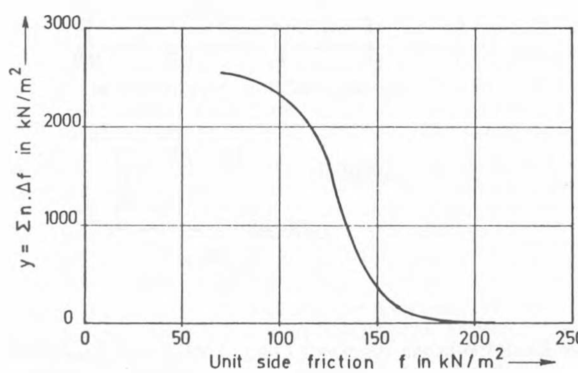

Fig.9 Cumulative curve of f in the sand of Kallo